Fabrication and Electro-photolysis Property of Carbon Nanotubes/Titanium Composite Photocatalysts for Methylene Blue

Feng-Jun Zhang,[†,‡] Ming-Liang Chen,[†] and Won-Chun Oh[†,*]

[†]*Department of Advanced Materials & Science Engineering, Hanseo University, Chungnam 356-706, Korea*
[*]*E-mail: wc_oh@hanseo.ac.kr*
[‡]*Anhui Key Laboratory of Advanced Building Materials, Anhui University of Architecture, Anhui Hefei 230022, P. R. China*
Received March 17, 2009, Accepted June 30, 2009

In this study, we have studied on improved performance of carbon nanotubes/titanium (CNT/TiO_2) structure electrode for methylene blue (MB). The composite electrodes consisting of CNTs and a titanium oxide matrix with phenol resin binder was fabricated with a mixture method. The chemical and morphological structure of CNT/TiO_2 composites were characterized by means of BET surface area, X-ray diffraction (XRD), scanning electron microscopy (SEM), UV-Vis absorption technique, Raman spectroscopy and energy dispersive X-ray (EDX). The electrode showed a remarkably enhanced performance for MB oxidation under UV illumination with or without electro-chemical reaction (ECR). Such a remarkably improved performance of the CNT/TiO_2 structure electrode might be due to the enhanced MB oxidation by electro- and photo-generated electrons and holes in the CNTs and TiO_2 under UV illumination with or without ECR.

Key Words: CNTs, Titanium dioxide, Electrode, Electrolysis, Photolysis

Introduction

Titanium dioxide, a large-band-gap semiconductor, is an excellent condidate as photocatalysts in the electro-oxidation of a wide variety of organic and inorganic substaces.[1] Titanium dioxide shows high adsorption ability to organic dye, corresponding with a high photocatalytic activity. TiO_2, as one of the semi conductive oxide, has been widely studied for its special photoelectric properties. In addition, TiO_2 is very stable in acidic solution and it has been reported that TiO_2 electrode has high catalytic activity and CO-tolerance for alcohol electro-oxidation.[2] Several modified methods have been reported to improve the photocataytic efficiency. These include increasing the surface area and efficiency of photocatalysts,[3] the generation of defect structures to induce space-charge separation,[4] and the modification of TiO_2 with metals[5,6] or other semiconductors and carbon materials.[7-10] Another method that might possibly increase the photocatalytic efficiency of TiO_2 is to add a co-sorbent such as silica, alumina, zeolites or clay and activated carbon.[11-14] The development of new materials for modifying TiO_2 system is urgently needed to increase the photocatalytic activity of TiO_2 for organic pollutant treatment.

In recent years carbon nanotubes (CNTs) have been widely explored in electrochemical studies,[15,16] mainly for microelectrode construction.[17] Microelectrodes prepared with CNTs material have good advantage due to their efficient radial mass transport properties leading to high sensitivity and short response time allowing for scanning. Another important advantage displayed by CNTs as electrodes is their high surface area containing acidic functional groups, which allow modification possibilities.[18,19] CNTs based electrodes attract considerable attention due to their special structure, extraordinary mechanical and unique electronic properties and potential applications. Their high mechanical strength makes them to be good candidates for advanced composites. They have either semiconducting, semimetallic or metallic, depending on the helicity and the diameter of the tube.[20] Such various properties open a promising field in nanoscale electrodevice applications. Thus, CNTs based electrode can be used as a promising system in the environmental cleaning. The application of CNTs electrode to enhance the photocatalytic activity of TiO_2 is proposed due to its superior photocatalytic (PC) ability compared with other photocataysts. In our study, CNTs were selected as the support materials for catalyst deposition in order to obtain a large surface area, better catalyst dispersion, and a resulting high electroactivity.

In this method, a positive potential was applied on the working electrode, which could inhibit the recombination of electrons and holes and enhance the rate of electrophotocatalytic (EPC) degradation of organic compounds.[21-23] The electrical driving force may play role in the sorption and decomposition of nonpolar molecules and metallic ions by creating obstacles for physical adsorption and prevent molecules from occupying the most energetically favorable positions on the carbon surface.[24,25] The purpose of this study is to propose synergentic effects of photolysis and electrolysis with CNT/TiO_2 electrode system by an electro-chemical method and to develop a new method to regenerate CNT/TiO_2 composite electrodes.

In this study, we have focused on the characterization of the CNT/TiO_2 composite electrodes prepared with weight ratio among CNT, anatase typed TiO_2 and phenolic resin binder. Moreover, the adsorption effects, structural variations, surface state and elemental compositions were investigated through preparation of three kinds of CNT/TiO_2 composites. We have studied the chemical and morphological structure of CNT/TiO_2 composites by means of BET surface area, X-ray diffraction (XRD), scanning electron microscope (SEM), UV-Vis absorp-

tion technique, Raman spectroscopy and energy dispersive X-ray (EDX). Finally, Methylene blue (MB, $C_{16}H_{18}N_3S{\cdot}Cl{\cdot}3H_2O$) solutions obtained from photolysis and electrolysis with CNT/TiO_2 electrode system by an electrochemical method were characterized by UV/Vis spectrophotometer.

Experimental

Materials. Crystalline multiwalled carbon nanotubes (CNTs) powder of 95.9 wt.% purity from Carbonnano (Carbonnano Co., Ltd. Korea) were used as a starting material. Reagents (benzene, tetrahydrofuran and ethyl alcohol) were purchased as reagent-grade from Duksan Pure Chemical Co and Daejung Chemical Co. and used without further purification unless otherwise stated. Methylene blue (MB, $C_{16}H_{18}N_3S{\cdot}Cl{\cdot}3H_2O$) was analytical grade and also purchased from Duksan Pure Chemical Co., Ltd. The novolac typed phenol resin was supplied from Kangnam Chemical Co. (Korea). The TiO_2 photocatalysts was commercially available (Duk-San Pure Chemical Co., Korea), which was composed of a single phase of anatase with secondary particles of about 80 ~ 150 μm aggregated from the primary particles of about 30 ~ 50 μm. This anatase-type titanium dioxide powder had a relatively large BET surface area of about 8.319 m^2/g.

Fabrication of electrodes. For the melting of phenol resin, ethyl alcohol was used as solvent. After desolving of phenol resin in the alcohol solution, TiO_2 powder and CNTs were mixed with resin-alcohol solution. And then, the mixtures were pressed into 9.95 × 39.5 × 5.95 mm hexagonal pellets in a mould. The curing temperature of the pelletized CNT/TiO_2 matrix was about 423 K. The cured samples were then pyrolyzed at 673 K for 1h in order to completely cure the binder. The nomenclatures of prepared samples were listed in Table 1.

Electrochemical characteristics. The CNT/TiO_2 composite matrix of test electrode was consisting of the size of 9.95 × 39.5 × 5.95 mm. The counter electrode of same size was artificial graphite (TCK, Korea). The initial MB solutions of 1.0×10^{-5} mole/L (c_0) were used as an electrolyte. The condition of electro-chemical reaction (ECR) for the measurements was 0.5 mA cm^{-2} with 3 V at room temperature.

Characterization of CNT/TiO_2 composites. For the characterization of CNT/TiO_2 composites, N_2 adsorption isotherm was measured at 77 K using a BEL sorp Analyzer (BEL, Japan). Then the BET surface area was calculated by nitrogen adsorption. SEM (JSM-5200 JOEL, Japan) was employed to observe the surface state and structure of the three kinds of CNT/TiO_2 composites. For the determination of the crystallographic structure of the composites, XRD patterns were taken using an X-ray generator (Shimatz XD-D1, Japan) with Cu Kα radiation. EDX spectra were also used for elemental analysis of the samples. For the analysis of the electrophotodegradation effects, UV-Vis spectra of the CNT/TiO_2 composites were recorded using a Genspec III (Hitachi, Japan) spectrometer.

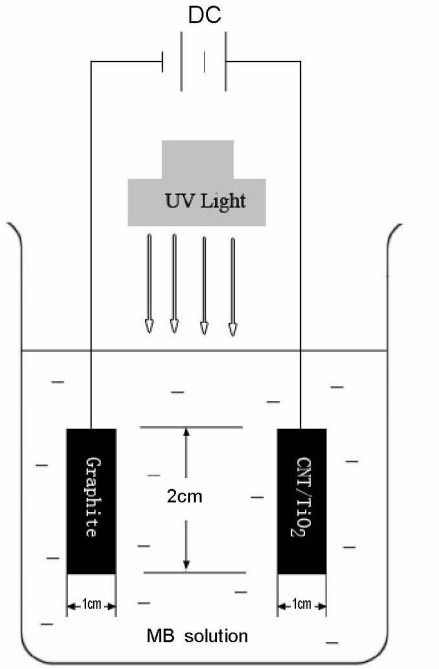

Figure 1. The sketch of EPC decomposition for MB solution with the CNT/TiO_2 electrode.

EPC effect. The EPC decomposition was performed with CNT/TiO_2 electrode and an aqueous solution of MB in a 100 mL glass container with ultraviolet (UV) light and with or without ECR. For UV irradiation, the ECR container was located axially and held in the UV lamp (20 W, 365 nm) box. The lamp was used at a distance of 100 mm from the solution in the darkness box. The c_0 was 1.0×10^{-5} mole/L. The EPC degradation of MB was performed with a potential voltage of 3.0 v and UV light (Fig. 1). The container was irradiated with UV light and operated with or without ECR as a function of irradiation time. MB solution degradaded were then withdrawn regularly from the reactor. The clean transparent solution was analyzed by UV/Vis spectroscopy. The concentration of MB in the solution was determined as a function of irradiation time from the absorbance region at a wavelength line of 660 nm.

Results and Discussion

Adsorption and surface properties. The CNT/TiO_2 composite catalysts fabricated with anatase, CNTs and phenol resin

Table 1. Nomenclatures of CNT/TiO_2 Composite Electrodes Prepared as Function of Preparation Condition

Preparation method	Nomenclatures
Carbon Nanotubes (50) + Titanium Dioxide (TiO_2 (99.99%), Anatase) (10) + Phenol Resin (Binder) (40)	CTPE1
Carbon Nanotubes (30) + Titanium Dioxide (TiO_2 (99.99%), Anatase) (30) + Phenol Resin (Binder) (40)	CTPE2
Carbon Nanotubes (10) + Titanium Dioxide (TiO_2 (99.99%), Anatase) (50) + Phenol Resin (Binder) (40)	CTPE3

*(Numerical Quantitiy): Weight Ratio (wt.%)

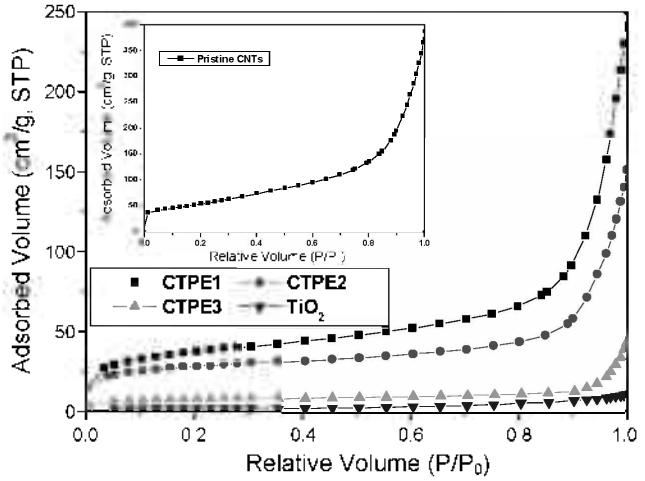

Figure 2. Nitrogen adsorption isotherms obtained from the pristine TiO_2, CNTs and CNT/TiO_2 composites.

Table 2. Textural Properties of CNT/TiO_2 Composite Samples

Sample	Parameter		
	S_{BET} (m^2/g)	Micropore Volume (cm^3/g)	Average Pore Diameter (nm)
TiO_2	8.319	0.0121	5.831
CNT	299.2	0.3496	7.114
CTPE1	135.1	0.2437	7.218
CTPE2	100.4	0.1112	4.432
CTPE3	28.86	0.0112	2.946

binder were noted as CTPE1, CTPE2 and CTPE3. Nitrogen adsorption isotherms for the pristine CNTs and three kinds of CNT/TiO_2 composites are shown in Fig. 2. The formation of Type II adsorption isotherms in these samples confirmed, which can be ascribed to one kind of reason for the containing of the majorly micropores and minorly mesopores on the surface of the composites. The adsorption volumes of CNT/TiO_2 composites studied decreased with an increase of TiO_2, which were mainly micro- and mesoporous in character with pore blocking and a minor presence of wider pores where capillary condensation occurred. The Table 2 shows the textural properties with microstructure changes of CNT/TiO_2 samples compared with pristine CNT and TiO_2. The BET surface areas of prestine TiO_2 and CNTs are 8.319 and 299.2 m^2/g, respectively, while those of composite catalysts decreased from 135.1 to 28.86 m^2/g with an increase of TiO_2 components. It is observed that the surface areas of composite catalysts are catastrophically reduced due to decreasing of CNTs components. Average pore diameter of different solids obtained from N_2 isotherm are also given in Table 2. Pores in multi walled CNT (MWCNT) include narrowly distributed inner hollow cavities of 3.4 nm and widely distributed aggregated pores of 20 nm formed by intercation of isolated MWCNT.[26] In this study, TiO_2 presents the average pore size at 5.831 nm. Average pore diameter of the MWCNT was 7.114 nm, which decreased greatly to about 4.432 and 2.946 nm when CTPE2 and CTPE3 composites were formed. It is considered that the

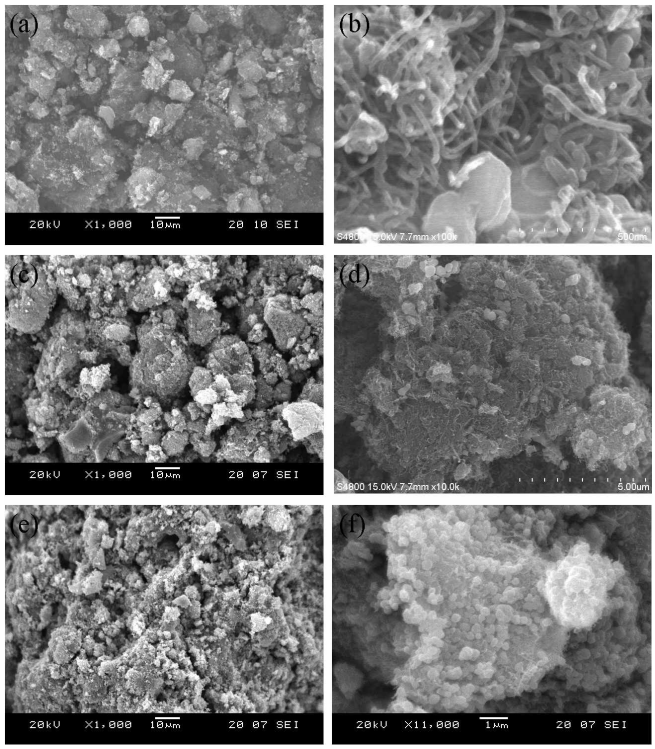

Figure 3. SEM and FE-SEM micrographs for the CNT/TiO_2 composites; (a) CTPE1 (over-all scale), (b) CTPE1 (close-up), (c) CTPE2 (over-all scale), (d) CTPE2 (close-up), (e) CTPE3 (over-all scale) and (f) CTPE3 (close-up).

average pore diameter is decreased a lot and it indicated that CNTs particles are homogenously distributed with TiO_2 particles. All of surface textural parameters for these composites were a considerably more decrease than that of pristine materials due to surface structural modification by an increase of TiO_2 components.

The micro-surface structures and morphology of the CNT/TiO_2 composites fabricated with anatase, CNTs and phenol resin binder were characterized by SEM and FE-SEM. The changes in the morphology for the CNT/TiO_2 composites obtained from our experimental condition are presented in Fig. 3. In case of CTPE1, it seems that a small amount of TiO_2 introduced into CNTs is distributed with TiO_2 particles from agglomerating. The particles of TiO_2 among the CNTs aggregated to be small clusters, and the aggregation was more evident of binding effect by phenol resin. This result (Fig. 3 (b)) is as well confirmed by FE-SEM inspection of CNT/TiO_2 composite materials. The image presents a close-up scale view of TiO_2 introduced from composite with external diameters ranging from 1.0 to 1.5 μm. In case of CTPE2 and CTPE3, it seems that a large amount of TiO_2 particles introduced into composites are distributed with a decrese of CNTs from agglomerating. It is observed that the pores for the composite matrix together with the interphaces between the agglomerates resulted in the appearance of meso or macropores. All samples have pores in their structures, which are connected randomly and lack discernible long-rang order in the pore arrangement. It is also found that, with the increase of

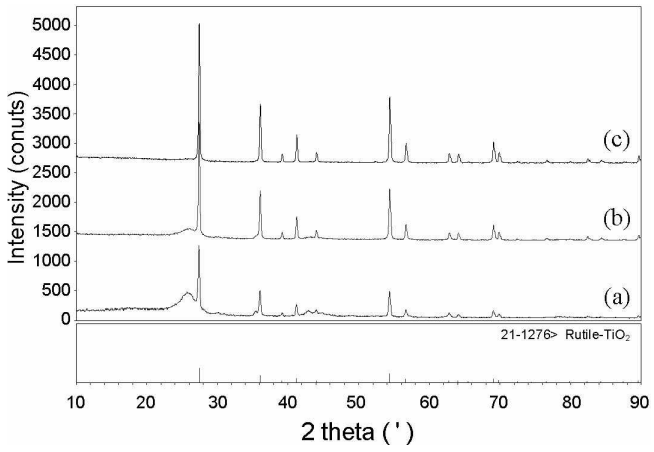

Figure 4. XRD patterns of the CNT/TiO_2 composites prepared with pristine CNTs and titanium dioxide: (a) CTPE1, (b) CTPE2 and (c) CTPE3.

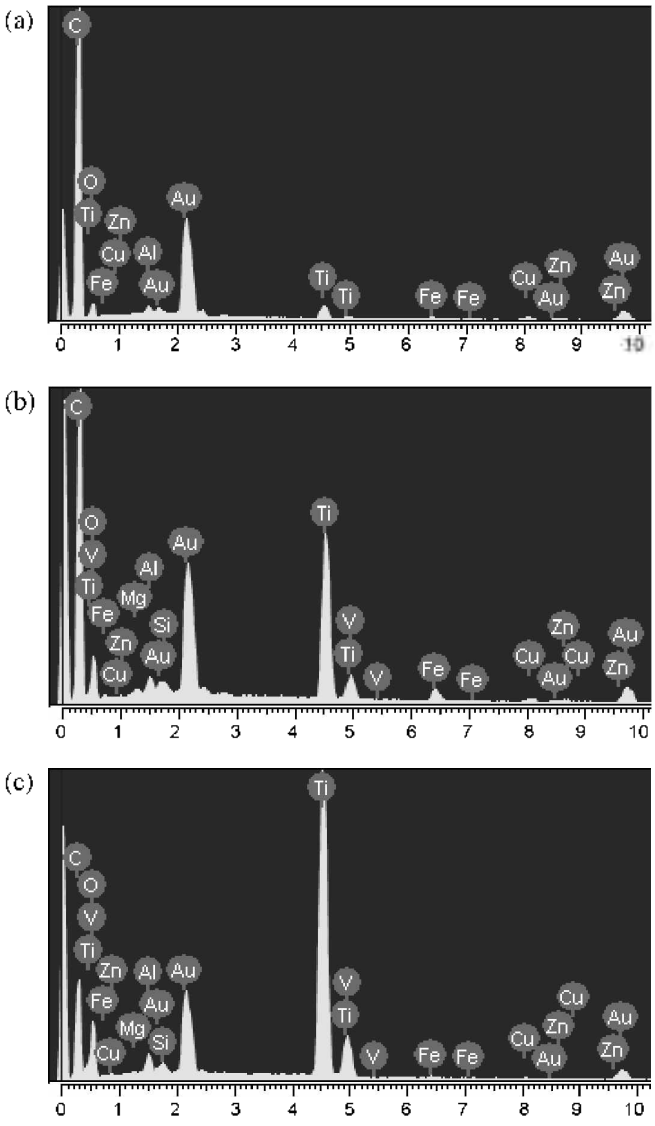

Figure 5. EDX elemental microanalysis for the CNT/TiO_2 composites: (a) CTPE1, (b) CTPE2 and (c) CTPE3.

the amount of CNTs, the morphology of TiO_2 changes from spherical particles (Fig. 3 (b), (d) and (f)), big agglomerated particles to bulk and there are more and more CNTs observed in the composites. By virtue of the composites with phenol resin being calsined, CNTs and TiO_2 particles were coherent each other, which formed the aggromerates with compact framework over the whole composites. However, the distribution of TiO_2 in the composites was not very uniform due to the controll of amount of CNTs or TiO_2 in fabrication process. Adding a few CNTs to the polymer matrix may signicantly enhance the emchanical properties.[27] However, the morphology state and mechanical properties of CNT/TiO_2 composites depend on the affinity of the filler to the phenol resin matrix.

Structural and chemical components. Fig. 4 showed the XRD patterns of three kinds of samples fabricated with CNTs, anatase and phenol resin binder. These results are presented the highly crystalline nature of the composites. The XRD results indicate that the phase transition from anatase phase to rutile phase has taken place at heat treated temperature (673 K). The most intense peaks of TiO_2 correspond to the rutile phases of (110), (101), (200), (211), (220), (311), and (112) at 28.1, 37.0, 89.1, 53.2, 55.2, 67.8 and 69.2 peaks. In case of CTP1 and CTP2, The one kind of intense peak of MWCNTs had presented to the (002) reflection. It is worth to notice that the intensity of CNTs diffraction peak increase from CTPE1 to CTPE3 and the width at half height of the peaks increases. This is consistent with the increasing amount of CNTs from CTPE1 to CTPE3. However, the diffraction peaks of MWCNTs were not clearly observed due to the relatively high intensity of TiO_2. Of the two crystal forms of TiO_2 catalysts, the anatase invariably exhibits a higher photoactivity than the rutile dose.[28,29] In contrast in our results, the results from Kominami *et al.*,[30] showed that the XRD patterns of TiO_2 derived from titanium alkoxide in organic solvents consistently presented the formation of anatase crystallites at low temperatures.

Elemental analyses of CNT/TiO_2 composites fabricated with CNTs, titanium dioxide and pheno resin binder were confirmed using EDX. Fig. 5 showed the spectra obtained from the CNT/TiO_2 composites. The spectra indicate the presence of C, O and Ti as major elements with small impurity metallic components. Additionally, the numerical result of quantitative EDX microanalysis of the CTPE1 yielded a component ratio of 81.3 : 10.4 : 2.68 for C : O : Ti. However, the results of the other case incresed for the Ti component with a decrease of the C component. In the case of most of the samples, C, Ti and O components were present as major elements in the CNT/TiO_2 composites. The results of the EDX elemental microanalysis (wt.%) of CNT/TiO_2 composites are listed in Table 3.

Table 3. EDX Elemental Microanalyses of CNT/TiO_2 Composites

Sample	Elements (wt.%)		
	C	O	Ti
CTPE1	81.3	10.4	2.68
CTPE2	56.9	18.9	17.3
CTPE3	26.6	33.5	36.8

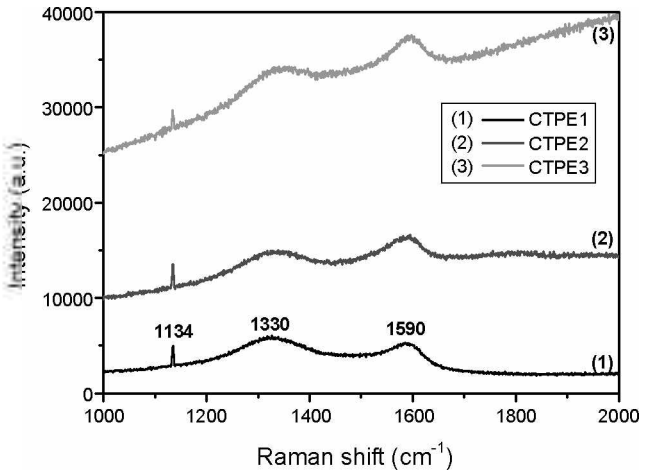

Figure 6. Raman spectra of the CNT/TiO_2 composites prepared with pristine CNTs and titanium dioxide.

Raman spectroscopy had been commenly applied discriminate the local order characteristics of CNTs. Fig. 6 showed the comparison of the Raman spectra of CTPE series in the wavenumber range between 1000 and 2000 cm^{-1}. There are three strong peaks at about 1134, 1330 and 1590 cm^{-1} in the samples of CNT/TiO_2 electrodes. The peak at 1330 cm^{-1} is assigned to the ill-organized graphite, the so-called D-line in CNTs.[31] The peak at around 1590 cm^{-1} is an unresolved Raman triplet identified with tangential carbon atom displacement modes, which is related to the E_{2g} mode in graphite.[32] The spectra of CNT/TiO_2 electrodes prepared are shown two strong peaks corresponding to the characteristic modes of MWCNTs. Another peak assigned at 1134 cm^{-1} can be attributed to the TiO_2 compound derived from titanium sources.

EPC effects for the MB. Fig. 7 shows the changes in relative concentration (c/c_0) of the MB concentration starting from 1×10^{-5} mol/L on the CNT/TiO_2 composites under UV irradiation in an aqueous solution. From the present results in Fig. 7(a), it can be seen that a PC process of MB with fast degradation efficiency was observed with an increase of the TiO_2 component. It is considered that the decreases of MB concentration in the aqueous solution can occurr in two physical phenomena such as adsorption by CNTs and photocatalytic decomposition by TiO_2, and that here it was mainly photocatalytic decomposition. As the result of EDX, the CTPE1 had the largest content of carbon and CTPE3 had the largest content of Ti. From the Fig. 7 (b), the EPC oxidation increased with an increase of CNT composition. According to former studies,[33,34] it is possible that catalytic decomposition of MB solution could be attributed to combined effects between TiO_2 photocatalytic activities, electro-assisted by CNTs. With an applied potential in the EPC, the recombination of photogenerated hole/electron pairs is suppressed by the externally applied electric field, and thus the life of the holes and electrons become longer.[35] so the conductivity of the CNT network facilitated the electron transfer between the adsorbed MB molecules and the catalyst substrate. This indicates that the decrease of MB can be concluded to be from combined effects of the photocatalytic decomposition by TiO_2 and

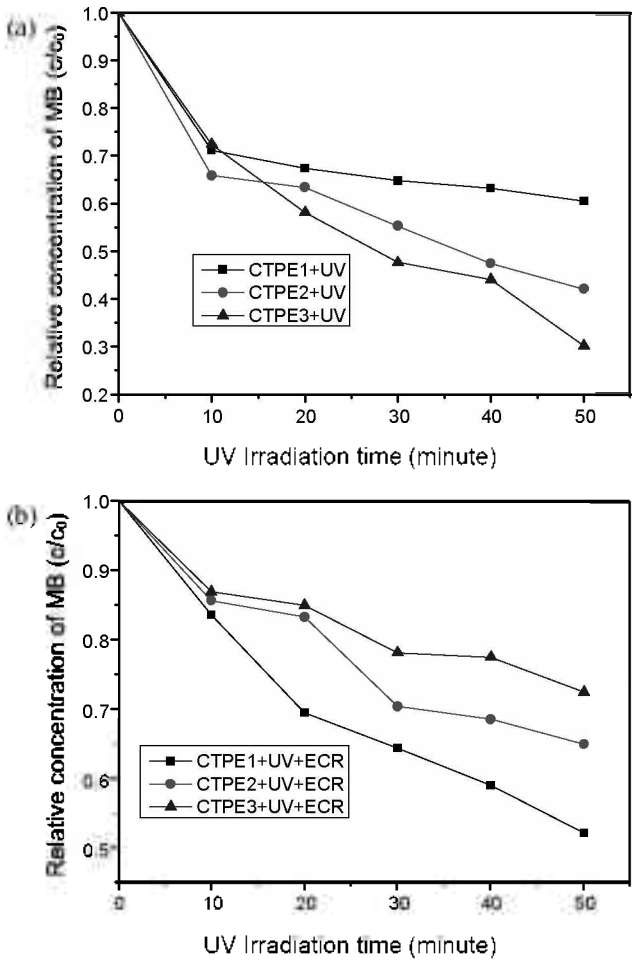

Figure 7. Dependence of relative concentration of MB in the aqueous solution C/C_0 after electrolysis and photolysis as time function with the CNT/TiO_2 composite electrodes.

electro-assistance from CNT network. As we known, it is general that CNTs have excellent electron conductivity. The characteristic electronic properties of CNTs are that they can be metallic as well as semiconducting depending on their geometry.

In order to study the optical response of samples, their UV-Vis absorption spectra were measured. Fig. 8, demonstrates the UV-Vis absorption spectra of the pristine TiO_2 and CNT/TiO_2 derivatives. The pristine TiO_2 display an absorption edge at about 345 nm. The blue shift of 42 nm might be attributed to the quantum confinement effect compared with that of former studied bulk anatase TiO_2 at 387 nm.[24,33] As shown in Fig. 8, it can be seen that CTPE series exhibit little absorption in the visible region. A noticeable red shift of absorption edge can be observed for these 3 kinds of samples in comparison with pristine one, which can be assigned to their crystal structure transformation from anatase to rutile after calcination at high temperature. This sensitivity for the light can be attributed to the mixed layer formed by CNT atoms. Increasing the CNT content increased the photocurrent, but it decreased when the CNT was increased further.[36] Although the undoped TiO_2 electrode provided a lower photocurrent than that of the CNT/TiO_2 sample, as a result of

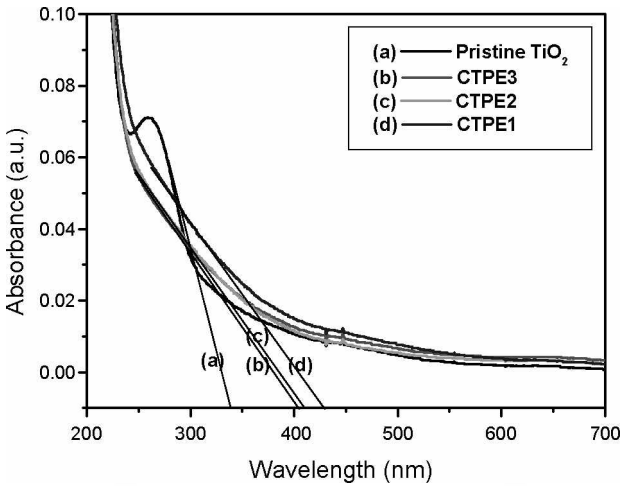

Figure 8. UV-Vis absorption spectra of the pristine TiO_2 and CNT/TiO_2 derivatives.

visible light absorption by residual carbon-containing and Ti^{3-} species. We believe there are three predominant explanations for the synergetic effect induced by the presence of the CNTs. First, the CNTs absorb over almost the entire visible light spectrum and act as photosensitizers, endowing the CNT/TiO_2 composites with an electron transfer mechanism similar to that of dye-sensitized TiO_2. Therefore, the CNT/TiO_2 samples can transfer excited electrons from the CNTs to the conduction band of TiO_2 when illuminated with visible light, thereby increasing the photocurrent. Second, the conductivity of CNTs is superior to that of TiO_2; therefore, we can expect a high transport rate of electrons in the CNT/TiO_2 composites. Third, the CNT/TiO_2 samples presumably possessed high surface areas, pore sizes, and pore volumes that enhanced visible light absorption and interfacial charge transfer, thereby improving the efficiency. On the other hand, an excess of CNTs may have decreased the crystallinity of the TiO_2 samples, thereby inhibiting the transport of electrons and increasing the probability of electron trapping by the crystal defects. Moreover, the shielding and scattering effects of excess CNTs might have prevented the photo absorption of other visible light-active species. Therefore, there is an optimal CNT loading at which the generated photocurrent was maximized.

CNTs have 1D carbon-based ideal molecule with the nanocylinder structures, which can conduct electricity at room temperature with essentially no resistance. This phenomenon is known as ballistic transport,[15] where the electrons can be considered as moving freely through the structure, without any scattering from atoms and defects. While the electron formed by the UV irradiation and electrical power migrate to the surface of TiO_2, it is easy for the electrons to transport in CNTs which are bound with TiO_2. The semiconducting properties of CNTs have been introduced the indubitable interaction between CNTs and TiO_2,[19] which may led to the higher catalytic activity by the process of the electron/hole pair formation under light irradiation. CNTs acting as electron sensitizer and donator in the composite photocatalysts may accept the electron (e^-) induced by light irradiation or ECR. The electrons in CNTs may be transfer into the conduction band in the TiO_2 particles. It is considered that photo-induced charge transfer occurs in the electronic interaction between the carbon layers or walls of CNTs and TiO_2. The electrons formed by the light irradiation or ECR on the surface of CNTs migrate to the surface of TiO_2 and thus they lead to the higher rate of the reduction of the e/h^+ pair recombination and the increase of the photon efficiency, which reduces the quantum yield of the TiO_2 catalyst. It has been confirmed that photo- or electro-induced charge transfer occurs in the electronic interaction between poymer chain and CNTs.[15] Since they connect well with each other and there is a strong interaction between CNTs and TiO_2, we can be proposed that e-transfer also happens in the CNT/TiO_2 composites, leading to the e^-/h^- recombination and the increase of the photon efficiency. The light absorption capability of photocatalyst and separation of photogenerated e^-/h^- pairs are crucial factors infulencing the photoactivity. Accordingly, it is more reasonable to ascribe that the electron absorptionability of CNT/TiO_2 composites greatly increases due to the more active sites available on the CNTs surface. Considering the semiconducting property of CNTs, it may absorb the irradiation and inject the photo- or electro-induced electrons into TiO_2 conduction band. These electrons in conduction band may react with O_2, which can be trigger the formation of very reactive superoxide radical ion (O_2^-). Simultaneously, a positive charged hole (h^-) might be formed with electron transfer from valence bond in TiO_2 to CNTs. The positive charged hole (h^-) may react with the OH^- derived from H_2O, which can be produced the hydroxyl radical (HO·). The more hydroxyl groups on the surface of photocatalysts, the more hydroxyl radical (HO·) will be produced by the oxidation of h^-.

Conclusion

We present the fabrication and characterization of CNT/TiO_2 composite electrodes consisting of CNTs and a titanium oxide matrix with phenol resin binder. The adsorption and surface properties, structural and chemical composition were investigated through preparation of the CNT/TiO_2 composites. Surface areas and pore volumes of CNT/TiO_2 samples were catastrophically reduced due to increasing of TiO_2 components. From the SEM results, all samples have pores in their structures, which are connected randomly and lack discernible long-rang order in the pore arrangement. In the XRD patterns, the diffraction patterns were certainly observed the transformed peaks from anatase to rutile phase. The EDX spectra revealed the presence of major elements such as C and O with strong Ti peaks. From the UV-Vis absorption spectra, a noticeable redshift of absorption edge can be observed for these 3 kinds of samples in comparison with pristine one. According to the photo catalytic results, the solution decomposed with the sample CTPE1 with UV and ECR appeared an excellent degradation effect with reaction time, due to the increase of electrical conductivity and electro-oxidation activity. It is considered that the decomposition of organic dye in the aqueous solution occur in synergetic effects such as photodecomposition and quantum efficiency by photo- and electro-induced electrons.

References

1. Si, S.; Huang, K.; Wang, X.; Chen, H. *Thin Solid Films* **2002**, *422*, 205.
2. Song, H.; Qiu, X.; Li, F. *Electrochem. Acta* **2008**, *53*, 3708.
3. Lakshminarasimhan, N.; Bae, E.; Choi, W. J. *Phys. Chem. C* **2007**, *111*, 15244.
4. Thurnauer, M. C.; Rajh, T.; Tiede, D. M. *Acta Chem. Scand.* **1997**, *51*, 610.
5. Yamashita, H.; Harada, M.; Misaka, J. *J. Photochem. Photobiol. A* **2002**, *148*, 257.
6. Xu, A. W.; Gao, Y.; Liu, H. Q. *J. Catal.* **2002**, *207*, 151.
7. Oh, W. C.; Bae J. S.; Chen, M. L. *Anal. Sci. Technol.* **2006**, *19*, 301.
8. Oh, W. C.; Bae, J. S.; Chen, M. L. *Bull. Korean Chem. Soc.* **2006**, *27*, 1423.
9. Oh, W. C.; Chen, M. L. *Bull. Korean Chem. Soc.* **2008**, *29*, 159.
10. Oh, W. C.; Bae, J. S.; Chen, M. L. *J. Ceram. Korean Soc.* **2008**, *45*, 196.
11. Matrails, H. K.; Ciardelli, M.; Ruwet, D. M. *J. Catalv.* **1995**, *157*, 368.
12. Chen, J.; Eberlein, L.; Langford, C. H. *J. Photochem. Photobio. A* **2002**, *148*, 183.
13. Oh, W. C.; Chen, M. L. *J. Ceram. Proc. Res.* **2008**, *9*, 100.
14. Oh, W. C.; Han, S. B.; Bae, J. S. *Anal. Sci. Technol.* **2007**, *20*, 279.
15. Cao, G. *Nanostructures & Nanomaterials*; Imperial College Press: 2004; pp 344-360.
16. Maiyalagan ,T. *Appl. Catal. B: Environ.* **2008**, *80*, 286.
17. Li, L.; Wu, G.; Xu, B. Q. *Carbon* **2006**, *44*, 2973.
18. Yadegari, H.; Jabbari, A.; Heli, H. *Electrochim. Acta* **2008**, *53*, 2907.
19. Yu, Y.; Yu, J. C.; Yu, J. G. *Appl. Catal. A General.* **2005**, *289*, 186.
20. Song, H.; Qiu, X.; Li, F.; Chen, L. *Electrochem. Commun.* **2007**, *9*, 1416.
21. Li, X. Z.; Liu, H. L.; Yue, P. T. *Sci. Technol.* **2000**, *34*, 4401.
22. Oliva, F. Y.; Avalle, L. B.; Santos, E.; C´amara, O. R. *J. Photochem. Photobiol. A: Chem.* **2002**, *146*, 175.
23. Oh, W. C.; Jung, A. R.; Ko, W. B. *J. Ind. Eng. Chem.* **2007**, *13*, 1208.
24. Oh, W. C.; Park, T. S. *J. Ind. Eng. Chem.* **2005**, *11*, 671.
25. Oh, W. C.; Lim, C. S. *J. Ceram. Proc. Res.* **2004**, *5*, 301.
26. Ndungu, P.; Godongwana, Z. G.; Petrik, L. F. *Synthesis of Carbon Nonostructured Materials Using LPG*: Microus and Mesoporous Materials, Internet Ed.: **2008**.
27. Tuen, S. M.; Ma, C. C.; Chung, C. Y. *Compos. Part. A* **2008**, *39*, 119.
28. Oh, W. C.; Bae, J. S.; Chen, M L. *Anal. Sci. Technol.* **2006**, *19*, 460.
29. Zhang, F. J.; Chen, M. L.; Oh, W. C. *Mater. Res. Soc. Korea* **2008**, *18*, 583.
30. Kominami, H.; Kato, J.; Takada,Y. *Catal. Lett.* **1997**, *46*, 235.
31. Tanaka, K.; Yamabe, T.; Fukui, K. *The Science and Technology of Carbon Nanotubes*; Elsevier Oxford: 1999; pp 51-61.
32. Dresselhous, M. S.; Dresselhous, G.; Avouris, P. *Carbon Nonotubes: Synthesis, Structure, Properties and Applications*; Springer: Berlin, 2001; pp 213-246.
33. Oh, W. C.; Jung, A. R. *J. Ceram. Korean. Soc.* **2008**, *45*, 150.
34. Oh, W. C.; Na, Y. R. *J. Ceram. Korean Soc.* **2008**, *45*, 36.
35. Oh, W. C.; Park, T. S. *Environ. Eng. Res.* **2007**, *12*, 218.
36. Chen, L. C.; Ho, Y. C.; Guo, W. S.; Huang, C. M.; Pan, T. C. *Electrochim. Acta* **2009**, *54*, 3884.